Corrugated metallodielectric superlattices via release-rollup assembly

N. Gibbons* **and J. J. Baumberg**

Cavendish Laboratory, University of Cambridge, CB3 0HE, UK

**ng322@cam.ac.uk*

Abstract: A 'release-rollup' assembly (RRA) technique is described that yields corrugated metallodielectric superlattices. Bilayers of polymer/Au cast onto diffraction gratings are released and rolled into multilayers with registration of the stacked corrugations across mm-scales. Optical imaging reveals Moiré fringes with reflection spectra that track the bilayer thickness due to mis-stacking. Angular-resolved spectra show spectrally-modulated diffraction opposite to that of the metallic stop-bands, but which agrees with a simple model. This scalable fabrication strategy is thus widely exploitable for laterally patterned metamaterials and optical superlattices.

OCIS codes: (230.4170) Multilayers; (220.4241) Nanostructure fabrication; (160.3918) Metamaterials; (160.5293) Photonic bandgap materials.

References and links

1. R. W. Wood, "'XLII. on a remarkable case of uneven distribution of light in a diffraction grating spectrum," Philos. Mag. **4**, 396–402 (1902).
2. U. Fano, "The theory of anomalous diffraction gratings and of quasi-stationary waves on metallic surfaces (Sommerfelds waves)," J. Opt. Soc. Am. **31**, 213–222 (1941).
3. M. B. Sobnack, W. C. Tan, N. P. Wanstall, T. W. Preist, and J. R. Sambles, "Stationary surface plasmons on a zero-order metal grating," Phys. Rev. Lett. **80**, 5667–5670 (1998).
4. Z. Chen, I. R. Hooper, and J. R. Sambles, "Strongly coupled surface plasmons on thin shallow metallic gratings," Phys. Rev. B **77**, 161405 (2008).
5. J. Le Perchec, P. Qumerais, A. Barbara, and T. López-Rios, "Why metallic surfaces with grooves a few nanometers deep and wide may strongly absorb visible light," Phys. Rev. Lett. **100**, 66408 (2008).
6. E. Popov, S. Enoch, and N. Bonod, "Absorption of light by extremely shallow metallic gratings: metamaterial behavior," Opt. Express **17**, 6770–6781 (2009).
7. J. Hao, J. Wang, X. Liu, W. J. Padilla, L. Zhou, and M. Qiu, "High performance optical absorber based on a plasmonic metamaterial," Appl. Phys. Lett. **96**, 251104 (2010).
8. R. A. Pala, J. White, E. Barnard, J. Liu, and M. L. Brongersma, "Design of plasmonic thin film solar cells with broadband absorption enhancements," Adv. Mater. **21**, 3504–3509 (2009).
9. M. Ghulinyan,C. J. Oton, Z. Gaburro, L. Pavesi, C. Toninelli, and D. S. Wiersma, "Zener tunneling of lightwaves in an optical superlattice," Phys. Rev. Lett. **94**, 127401 (2005).
10. M. J. Bloemer and M. Scalora, "Transmissive properties of Ag/MgF photonic band gaps," Appl. Phys. Lett. **72**, 1676 (1998).
11. N. Gibbons, J. J. Baumberg, C. L. Bower, M. Kolle, and U. Steiner, "Scalable cylindrical metallodielectric metamaterials," Adv. Mater. **21**, 3933–3936 (2009).
12. R. S. Bennink, Y. K. Yoon, R. W. Boyd, and J. E. Sipe, "Accessing the optical nonlinearity of metals with metal-dielectric photonic bandgap structures," Opt. Lett. **24**, 1416–1418 (1999).
13. N. N. Lepeshkin, A. Schweinsberg, G. Piredda, R. S. Bennink, and R. W. Boyd, "Enhanced nonlinear optical response of one-dimensional metal-dielectric photonic crystals," Phys. Rev. Lett. **93** (12), 123902 (2004).
14. B. Wood, J. B. Pendry, and D. P. Tsai, "Directed subwavelength imaging using a layered metal-dielectric system," Phys. Rev. B **74**, 115116 (2006).
15. Anan Fang, Thomas Koschny, and Costas M. Soukoulis, "Optical anisotropic metamaterials: negative refraction and focusing," Phys. Rev. B **79** (24), 245127 (2009).

#145564 - $15.00 USD Received 7 Apr 2011; revised 7 Jun 2011; accepted 9 Jun 2011; published 29 Jul 2011

16. Z. Liu, H. Lee, Y. Xiong, C. Sun, and X. Zhang, "Far-field optical hyperlens magnifying sub-diffraction-limited objects," Science **315**, 1686 (2007).
17. C. C. Fu, A. Grimes, M. Long, C. G. L. Ferri, B. D. Rich, S. Ghosh, L. P. Lee, A. Gopinathan, and M. Khine, "Tunable nanowrinkles on shape memory polymer sheets," Adv. Mater. **21**, 4472–4476 (2009).
18. W. T. S. Huck, "Artificial skins: hierarchical wrinkling," Nat. Mater. **4**, 271–272 (2005).
19. K. Efimenko, M. Rackaitis, E. Manias, A. Vaziri, L. Mahadevan, and J. Genzer, "Nested self-similar wrinkling patterns in skins," Nat. Mater. **4**, 293–297 (2005).
20. O. Schumacher, S. Mendach, H. Welsch, A. Schramm, C. Heyn, and W. Hansen, "Lithographically defined metal-semiconductor-hybrid nanoscrolls," Appl. Phys. Lett. **86**, 143109 (2005).
21. S. Schwaiger, M. Brll, A. Krohn, A. Stemmann, C. Heyn, Y. Stark, D. Stickler, D. Heitmann, and S. Mendach, "Rolled-up three-dimensional metamaterials with a tunable plasma frequency in the visible regime," Phys. Rev. Lett. **102** (16), 163903 (2009).
22. S. P. Lacour, S. Wagner, Z. Huang, and Z. Suo, "Stretchable gold conductors on elastomeric substrates," Appl. Phys. Lett. **82**, 2404 (2003).
23. F. Huang, J.J. Baumberg, "Actively tuned plasmons on elastomerically driven Au nanoparticle dimers," Nano Lett. **10**, 1787–1792 (2010)
24. I.M. Pryce, K. Aydin, Y. A. Kelaita, R. M. Briggs, and H. A. Atwater, "Highly strained compliant optical metamaterials with large frequency tunability," Nano Lett. **10**, 4222–4227 (2010)
25. M. Kolle, B. Zheng, N. Gibbons, J. J. Baumberg, and U. Steiner, "Stretch-tuneable dielectric mirrors and optical microcavities," Opt. Express **18**, 4356 (2010).
26. M. D. Austin, H. Ge, W. Wu, M. Li, Z. Yu, D. Wasserman, S. A. Lyon, and S. Y. Chou, "Fabrication of 5 nm linewidth and 14 nm pitch features by nanoimprint lithography," Appl. Phys. Lett. **84**, 5299 (2004).
27. V. M. Shalaev, W. Cai, U. K. Chettiar, H. K. Yuan, A. K. Sarychev, V. P. Drachev, and A. V. Kildishev, "Negative index of refraction in optical metamaterials," Opt. Lett. **30**, 3356 (2005).

1. Introduction

Grating structures have applications in many areas of optics including spectroscopy, distributed feedback lasers, and wavelength multiplexers and demultiplexers. Metallic gratings hold particular interest as they exhibit angularly- and spectrally-sharp reflection features arising from Wood's anomalies [1] and surface plasmons. These resonances were first linked to the idea of electromagnetic surface waves by Fano [2] and they have since been studied extensively [3, 4]. Metamaterial grating structures with subwavelength groove spacing or depth have also been investigated as a route to achieving close to 100% absorption or reflection of incident light [5–7]. Such an effect arises when the grating depth is an order of magnitude smaller than the wavelength of the incident light and the excitation of surface plasmon polaritons in the electrostatic regime leads to near-perfect absorption. Such a property is of particular appeal in plasmonic solar cells [8].

Incorporating periodic gratings within a Metallodielectric Distributed Bragg Reflector (MDBR) structure introduces an additional set of resonances due to the Fabry-Perot modes which exist within the multilayer. Such planar metallodielectric structures with periodically spaced 10nm-scale metal layers have many unusual optical properties in the Bragg regime (wavelength-scale spacing) such as forming superlattices with optical minibands (exhibiting Bloch oscillations and Zener tunnelling [9]), showing resonant optical transmission (several thousand times that in equivalent thickness of bulk metal [10, 11]) and significantly enhanced nonlinear optical properties [12, 13] due to the ultrafast changes in the refractive index of the ultrathin metal layers, making them of interest for optical switching. When arranged in a metamaterial configuration (subwavelength spacing) their properties can include negative refraction, anisotropic propagation and hyperlensing [14–16].

In this paper we demonstrate a scalable manufacturing process and optical response of corrugated metallodielectric superlattices by combining thin metal structures with polymers, using stacked corrugations as an exemplar to demonstrate the photonic properties and their interplay with the structural assembly. Fabrication of such corrugated layers with standard inorganic materials depends on traditional layer-by-layer lithography. Previous approaches for soft materials

#145564 - $15.00 USD Received 7 Apr 2011; revised 7 Jun 2011; accepted 9 Jun 2011; published 29 Jul 2011

have used strain, either prestraining polymer layers before metal coating [17], or cross-linking the upper polymer layer with UV/oxygen plasma [18,19], which wrinkle when released to form periodic corrugations. These approaches offer only limited flexibility and thus have not been adopted for multilayer gratings.

2. Fabrication

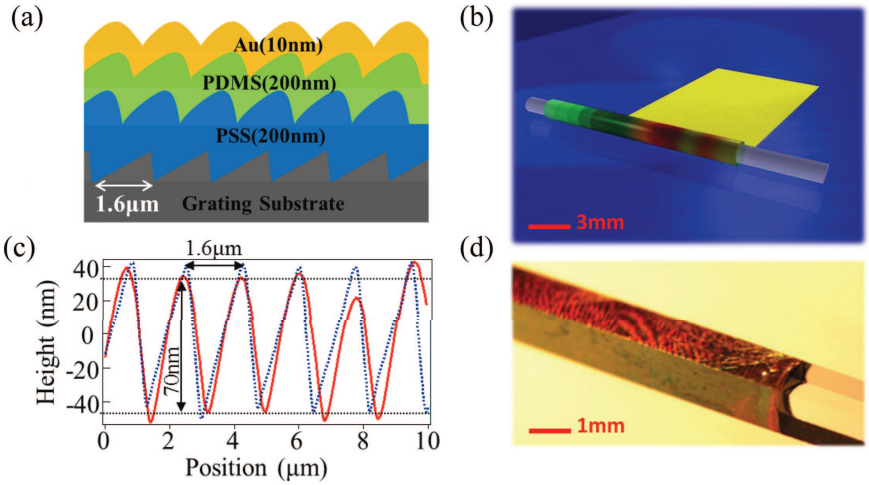

Fig. 1. (a) Bilayer cross-section after Au deposition on PSS and PDMS layers spin-coated onto a 1.6μm pitch grating. (b) Corrugated bi-layer of Au/PDMS released from the substrate and rolled up around a silica rod of width 1.5mm. (c) AFM scan across rolled-up sample (red), and original grating (height÷3, blue dashed). (d) Photo of a 4-bilayer grating MDBR. Surface Moiré fringes arise from imperfect groove alignment.

The fabrication method adopted here is to form the basic repeat layers of the structure incorporating the lateral grating, and then to stack these layers around a central silica rod using what we term *release-rollup assembly* (RRA). This approach can avoid typical problems of non-conformity between layers, long fabrication times, and planarisation of layer features with increased number of layers [11]. While previous work has utilised semiconductor strain mismatch to self-roll metallo-semiconductor multilayers [20] and metamaterials [21], our approach offers much greater freedom in material choices, specifically the use of flexible dielectrics. A diffraction grating with pitch a=1.6μm and 750nm blaze is used as the lateral structure template and is first spin-coated with a solution of polysulfonic acid (PSS, Sigma Aldritch), which is a water soluble polymer used as the sacrifical release layer [Fig. 1(a)]. The sample is then spin-coated with 200nm of elastomeric polymethylsiloxane (PDMS, Dow Corning, Sylgard 184) and cured at 120°C for 2 hours to crosslink the polymer chains. To complete the metallodielectric bilayer 15nm of gold is vacuum evaporated onto the PDMS surface. By utilising the solubility of the PSS layer, the corrugated metallodielectric bilayer is floated off the grating substrate in a bath and supported easily upon a water surface due to the large hydrophobicity of PDMS and high surface tension of water. Once floating, the bilayer can be rolled around a square or circular cross-section silica rod to form a multilayer [Fig. 1(b)]. We note that rolls with more than 100 layers have already been produced using this technique. Here grating areas of 3×3cm with a square rod of 1.5mm cross-section yield up to 4 bilayers, although this

#145564 - $15.00 USD Received 7 Apr 2011; revised 7 Jun 2011; accepted 9 Jun 2011; published 29 Jul 2011

can be easily scaled up [11]. Atomic Force Microscopy (AFM) is used to track the surface profile after the deposition of each successive bilayer component. The grating amplitude and blaze decrease after each successive deposition. While the initial grating amplitude is 400nm, after coating with PSS, PDMS and Au layers this amplitude reduces to 20nm. However, once the film is released from the substrate and rolled around the central rod the amplitude increases again to 70nm [Fig. 1(c)]. This is due to relaxation of the strain produced in the layer deposition process. It is clear that the asymmetric blaze also decreases in the deposition process. Further optimisation can better preserve the original grating shape. Additionally, the grating depth can be influenced directly by the template depth and indirectly by the thickness of the sacrificial layer.

3. Stacking dynamics

A photograph of the grating MDBR [Fig. 1(d)] shows the resulting high optical quality. The alignment of successive layers of the grooves can be directly observed by imaging. Domains of greater than 1mm size can be easily produced, implying locking of the overlying gratings over $\geq$ 1000 periods. The evident Moiré fringes in samples such as Fig. 1(d) arise from slight angular misalignment between corrugations in successive layers. These are more clearly observed in dark field micrographs [Fig. 2(a)] in which diffracted light from off-normal incidence is collected. The groove mismatch mechanism which lies behind the formation of these fringes is shown in Fig. 2(b). High magnification images at different positions are shown in Fig. 2(c). Regions in which the gratings are vertically stacked coherently increases the diffraction intensity leading to bright regions (B), while areas in which the gratings are staggered are disordered and show less diffraction (D). These fringes thus map the registration of the grooves, offering insight into the meshing process and allowing us to conveniently characterise the entire sample surface area.

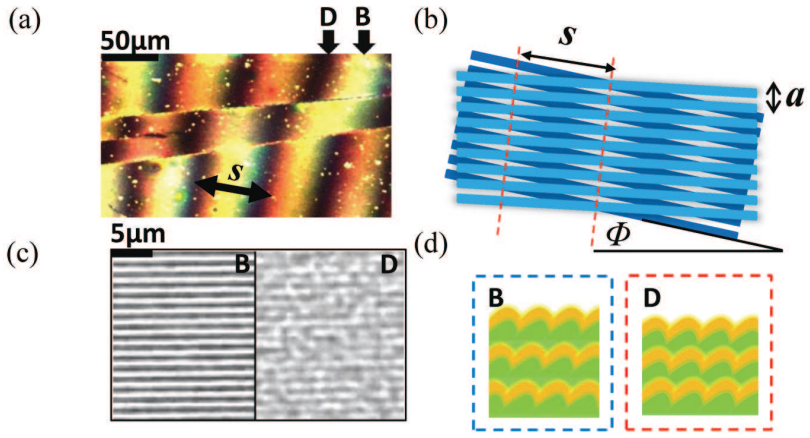

Fig. 2. (a) Dark field image showing Moiré fringes caused by groove misalignment. (b) Bright field images showing surface grooves at areas of good (B) and poor (D) registration. (c) Small groove mismatch angles, θ, lead to Moiré fringes of spacing, s. (d) Different registration configurations arise from groove mismatch.

The mismatch angle, θ, between two overlying gratings can be extracted from the images as $\sin\theta = a/s$, where s is the measured Moiré fringe spacing [Fig.2(b)]. For the present RRA, mismatches of θ=0° to 2° are found. Observed jumps in mismatch angle are caused by lat-

#145564 - $15.00 USD Received 7 Apr 2011; revised 7 Jun 2011; accepted 9 Jun 2011; published 29 Jul 2011

eral shifts of the overlayer or slight changes in the rolling angle from wrinkling, producing a sudden change in the separation of the fringes or their phase. This behaviour suggests that a groove-locking mechanism operates across the surface. Areas where the grooves do not mesh efficiently are flattened and distorted due to strain, leading to a stretching of the flexible polymer layers and a decrease in their effective thickness [Fig. 2(d)]. Characteristic bright-field spectra taken on the bright (B) and dark (D) fringes [Fig. 3(a)] display the Bragg stopbands expected from these MDBRs [11]. However the spectra from the dark fringes are slightly blue-shifted and this effect is consistently repeated across all the dark fringes. A similar spectral evolution is obtained from transfer matrix simulations [Fig. 3(b)] of 3-layer metallodielectric DBRs with slightly varying polymer thickness. The spectrum is blue-shifted as the polymer thickness is decreased and the stopband drops in intensity. This spectral shift is due to the slight flattening of the dielectric layer described previously [Fig. 2(d)]. Simulations suggest that the maximum change in effective thickness is ≈4%. As the number of layers increases more complex stacking geometries arise, however our simulations indicate that the upper two layers substantially influence the Moiré fringe response, supporting this intuitive analysis.

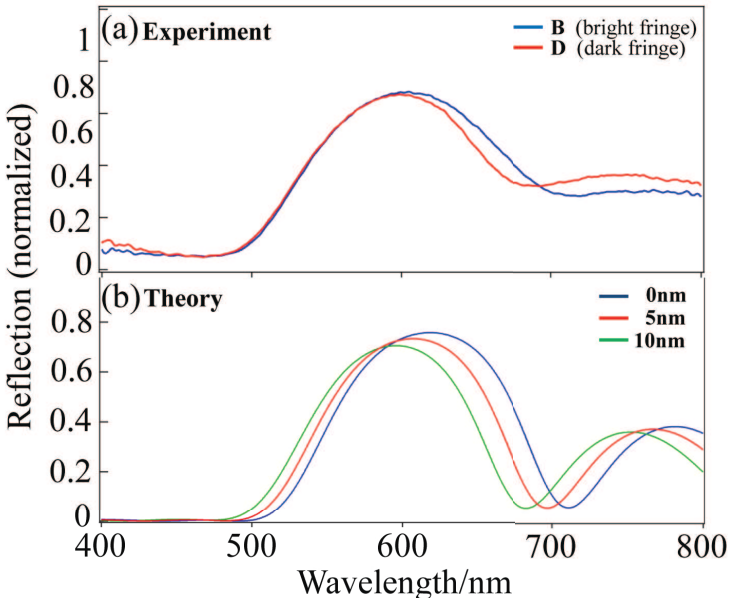

Fig. 3. (a) Bright field spectra from adjacent dark (D) and bright fringes (B) with collection spot size of 5μm. (b) Corresponding transfer matrix simulations of flat multilayers with varying polymer thickness.

4. Spectrally structured diffraction

To better understand this stacking, angle-resolved spectra of 2 grating MDBRs are taken using an automated goniometer illuminated by an unpolarized white light laser source focused to a 250μm spot to measure the sample diffraction [Fig. 4(a)]. The light is normally incident and the detector angle varied across 60° to collect the reflected and ±1 diffracted orders [Fig. 4(b)]. The reflection spectrum of 2 and 3 bilayers is well-accounted for by transfer matrix simulations of planar structures consisting of 200nm of PDMS and 15nm gold in each bilayer. These simulations show only a weak polarization dependence due to the significant Au reflectivity of each

#145564 - $15.00 USD Received 7 Apr 2011; revised 7 Jun 2011; accepted 9 Jun 2011; published 29 Jul 2011

layer. Extracting the intensities from the different diffractive orders from 2 bilayers [Fig. 4(c)] and 3 bilayers [Fig. 4(d)] shows that diffraction is *enhanced* at wavelengths of *minimum* Bragg reflection. Hence the vertical grating stack spectrally structures the diffractive response.

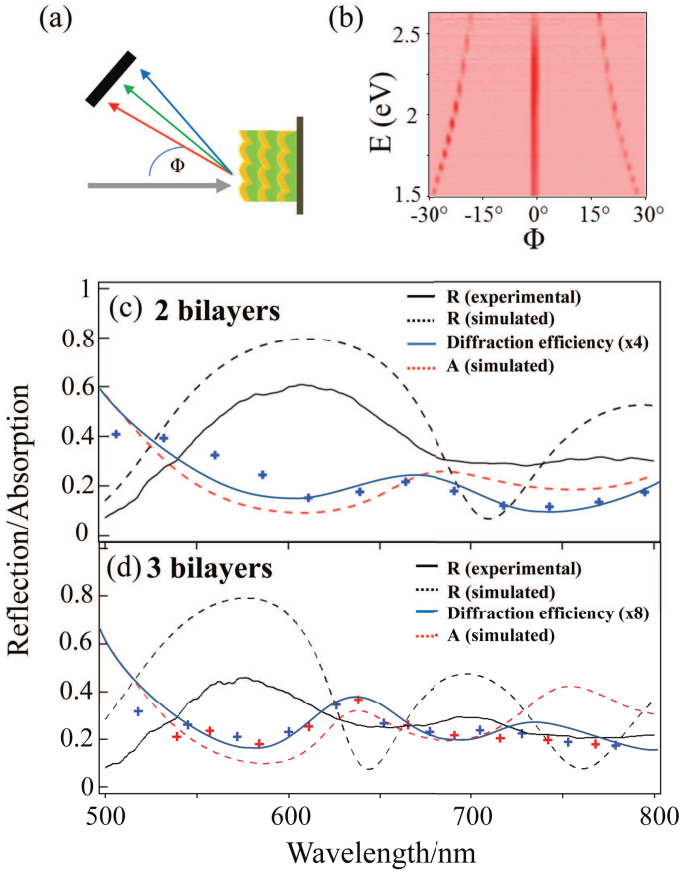

Fig. 4. (a) Schematic white-light goniometer rig. (b) Intensity from corrugated multilayer measured at different collection angles with 0° incidence. (c) Reflection spectrum (•) with corresponding simulation of flat MDBR (black dashed). Extracted diffraction intensities of +1 (blue +) order (×8) plotted along with simulated MDBR absorption (red dashed). Shown for 2 bilayers and, (d) 3 bilayers for +1 (blue +) and -1 (red +) diffractive orders.

To account for these effects, we plot the absorption within the multilayer for light emerging at 20° (which is the diffraction angle within the sample for $\lambda \simeq$600nm) [Fig. 4(c) and 4(d), red dashed]. At the DBR mode dips which correspond to the modes of the optical superlattice [9], light penetrates deeper into the sample through the miniband modes and the optical field within the Au layers is largest. Diffraction occurs primarily at the gold interfaces and therefore it is maximised when the field intensity here is at its highest, thus accounting for the observed spectrally-modulated diffraction efficiency. The diffraction enhancement effects described here tune with the geometry of the sample and its stopband, as seen in Fig. 4(c) and 4(d) for 2 and 3 bilayer samples. The diffraction resonance blue-shifts in concert with the spectral position of the first absorption peak as expected from the current model.

#145564 - $15.00 USD Received 7 Apr 2011; revised 7 Jun 2011; accepted 9 Jun 2011; published 29 Jul 2011

Registration of these corrugated bilayers can be further improved through the use of alternative polymers which have lower adhesion to gold, encouraging better groove alignment. An advantage of PDMS however is its flexbility, which opens the door to stretch-tuneable metallic devices. Related stretchable metallic structures have been investigated as a route towards flexible electronics [22], flexible plasmonics [23] and flexible metamaterials [24]. By using a PDMS rod or fibre to roll the corrugated film, the whole structure can be stretched as one. Although Au sheets are mechanically rigid, the corrugation of the gold layer now allows transverse compression and stretching (perpendicular to the rod axis). This leads to 'concertina' expansion of the layers and an increase in grating pitch. Hence the plasmonic response of such a nanostructure can be actively tuned simply and with no hysterisis. We have recently reported a similar technique to stretch-tune purely dielectric elastomeric DBRs and microcavities [25].

5. Discussion

In conclusion, we demonstrate an effective approach to the fabrication of metallodielectric grating structures which avoids the requirement of multiple depositions and provides good overall groove registration. Most importantly this process is entirely scalable. The diffractive properties of the grating MDBRs are modulated in accordance with the resonant absorption within the gold layers. The sub-100nm groove depth demonstrated here can be easily reduced, and we have already achieved polymer layer thicknesses below 50nm. Incoporating lateral periodicity into such optical superlattices now allows a variety of new effects including real-time control and modification of Zener tunnelling within the minibands, as well as a range of other miniband devices. Metallodielectric multilayers with such subwavelength dimensions can support the evanescent components of an image through their coupling with plasmonic modes and anisotropic propagation through the stack [14, 15]. Such properties can ultimately lead to subwavelength imaging and our grating structures can allow these plasmon modes to be explored through direct diffractive coupling from the corrugated layers. Lateral periodicity of sub-50nm is also straightforward (independent of the materials used) enabling truly subwavelength-scale structuring [26]. Another intriguing possibility is the formation of periodic arrays of metallic rods or strips within the grooves of the grating by a single angled evaporation onto the corrugated surface. Subsequent roll-up would allow control over the nanorod periodicity due to the groove registration effect we have reported. Similar configurations have been shown to exhibit unique plasmonic and electromagnetic properties such as a negative index of refraction [27].

Acknowledgments

This work was supported by EPSRC EP/G060649/1, EP/F059396 and Kodak.

#145564 - $15.00 USD Received 7 Apr 2011; revised 7 Jun 2011; accepted 9 Jun 2011; published 29 Jul 2011